Short and robust directional couplers designed by shortcuts to adiabaticity

Shuo-Yen Tseng,[1,2] **Rui-Dan Wen,**[3] **Ying-Feng Chiu,**[1] **and Xi Chen**[3,*]

[1]*Department of Photonics, National Cheng Kung University, Tainan, Taiwan*
[2]*Advanced Optoelectronic Technology Center, National Cheng Kung University, Tainan, Taiwan*
[3]*Department of Physics, Shanghai University, 200444 Shanghai, China*
[*]*xchen@shu.edu.cn*

Abstract: We propose short and robust directional couplers designed by shortcuts to adiabaticity, based on Lewis-Riesenfeld invariant theory. The design of directional couplers is discussed by combining invariant-based inverse engineering and perturbation theory. The error sensitivity of the coupler is minimized by optimizing the evolution of dynamical invariant with respect to coupling coefficient/input wavelength variations. The proposed robust coupler devices are verified with beam propagation simulations.

OCIS codes: (000.1600) Classical and quantum physics; (060.1810) Buffers, couplers, routers, switches, and multiplexers; (130.3120) Integrated optics devices; (130.2790) Guided waves.

References and links

1. A. Syahriar, V. M. Schneider, and S. Al-Bader, "The design of mode evolution couplers," J. Lightwave Technol. **16**, 1907–1914 (1998).
2. T. A. Ramadan, R. Scarmozzino, and R. M. Osgood, "Adiabatic couplers: design rules and optimization," J. Lightwave Technol. **16,** 277–283 (1998).
3. X. Sun, H.-C. Liu, and A. Yariv, "Adiabaticity criterion and the shortest adiabatic mode transformer in a coupled-waveguide system," Opt. Lett. **34,** 280–282 (2009).
4. R. R. A. Syms, "The digital directional coupler: improved design," IEEE Photon. Technol. Lett. **4,** 1135–1138 (1992).
5. G. T. Paloczi, A. Eyal, and A. Yariv, "Wavelength-insensitive nonadiabatic mode evolution couplers," IEEE Photon. Technol. Lett. **16,** 515–517 (2004).
6. S.-Y. Tseng, "Counterdiabatic mode-evolution based coupled-waveguide devices," Opt. Express **21,** 21224–21235 (2013).
7. S. Longhi, "Quantum-optical analogies using photonic structures," Laser and Photon. Rev. **3,** 243–261 (2009).
8. E. Torrontegui, S. Ibáñez, S. Martínez-Garaot, M. Modugno, A. del Campo, D. Guéry-Odelin, A. Ruschhaupt, X. Chen, and J. G. Muga, "Shortcuts to adiabaticity," Adv. At. Mol. Opt. Phys. **62,** 117–169 (2013).
9. T.-Y. Lin, F.-C. Hsiao, Y.-W. Jhang, C. Hu, and S.-Y. Tseng, "Mode conversion using optical analogy of shortcut to adiabatic passage in engineered multimode waveguides," Opt. Express **20,** 24085–24092 (2012).
10. S.-Y. Tseng and X. Chen, "Engineering of fast mode conversion in multimode waveguides," Opt. Lett. **37,** 5118–5120 (2012).
11. S. Martínez-Garaot, S.-Y. Tseng, and J. G. Muga, "Compact and high conversion efficiency mode-sorting asymmetric Y junction using shortcuts to adiabaticity," Opt. Lett. **39**, 2306 (2014).
12. X. Chen and J. G. Muga, "Engineering of fast population transfer in three-level systems," Phys. Rev. A **86**, 033405 (2012).
13. S.-Y. Tseng and Y.-W. Jhang, "Fast and robust beam coupling in a three waveguide directional coupler," IEEE Photon. Technol. Lett. **25**, 2478–2481 (2013).
14. A. Ruschhaupt, X. Chen, D. Alonso, and J. G. Muga, "Optimally robust shortcuts to population inversion in two-level quantum systems," New J. Phys. **14,** 093040 (2012).
15. D. Daems, A. Ruschhaupt, D. Sugny, and S. Guérin, "Robust quantum control by a single-shot shaped pulse," Phys. Rev. Lett. **111**, 050404 (2013).

#214031 - $15.00 USD Received 13 Jun 2014; revised 17 Jul 2014; accepted 18 Jul 2014; published 28 Jul 2014

16. X.-J. Lu, X. Chen, A. Ruschhaupt, D. Alonso, S. Guérin, and J. G. Muga, "Fast and robust population transfer in two-level quantum systems with dephasing noise and/or systematic frequency errors," Phys. Rev. A **88,** 033406 (2013).
17. X. Chen, E. Torrontegui, and J. G. Muga, "Lewis-Riesenfeld invariants and transitionless quantum driving," Phys. Rev. A **83,** 062116 (2011).
18. H. R. Lewis and W. B. Riesenfeld, "An exact quantum theory of the time-dependent harmonic oscillator and of a charged particle in a time-dependent electromagnetic field," J. Math. Phys. **10,** 1458–1473 (1969).
19. C.-L. Chen, *Foundations for Guided-Wave Optics* (Wiley, 2007).
20. K. Kawano and T. Kitoh, *Introduction to Optical Waveguide Analysis: Solving Maxwell's Equations* (Wiley, 2001).
21. K. Okamoto, *Fundamentals of Optical Waveguides* (Academic, 2006).
22. D. R. Rowland, Y. Chen, and A. W. Snyder, "Tapered mismatched couplers," J. Lightwave Technol. **9,** 567–570 (1991).

1. Introduction

The directional coupler is one of the most important devices in integrated optics. Couplers with tolerance to variations in fabrication and wavelength are of extreme interest in optical communications. The adiabatic couplers do not require strict fabrication control and have the desired broadband characteristics. The operation principle of adiabatic couplers is based on the evolution of a single waveguide local mode (supermode) that is caused by the gradual change in the device geometry, and coupling between the supermodes are negligible when the adiabatic condition is met. So, the adiabatic coupler generally requires a longer device length. There have been attempts to obtain the optimal design of adiabatic couplers by choosing optimized shape functions [1, 2], in which the coupled-mode equations describing coupling between the unperturbed waveguide modes are solved by numerical integration using different shape functions. The other approach is to find the optimal shape function that minimizes the coupling between the supermodes [3]. These approaches are based on the adiabatic approximation; as long as there is finite coupling between the supermodes, the coupling efficiency will only be unity at specific operating points [4, 5]. On the other hand, one could obtain adiabatic-like bandwidth and fabrication tolerance by the addition of a counter-diabatic couping term in the design to cancel all unwanted coupling between the supermodes [6]. This approach guarantees a perfect coupling, because all unwanted supermodes coupling has been cancelled. However, the counter-diabatic term is strictly related to the chosen shape function, and one can only optimize the device characteristics through repeated iteration with various shape functions.

Recently, many coherent quantum phenomena have been exploited to implement light manipulation in waveguide structures based on the analogies between quantum mechanics and wave optics [7]. At the same time, the development in new ways to manipulate quantum systems with high-fidelity and in a short interaction time using the so called "shortcuts to adiabaticity" approaches [8] also sheds light on the design of novel coupled-wave devices [6,9–11]. In particular, the invariant-based inverse-engineering approach [12] provides a versatile toolbox for designing short waveguide couplers [13], in terms of dynamical modes of the invariant. In addition to accelerating slow adiabatic passage, the invariant-based approach also provides an efficient way to analyze the system stability versus different types of perturbations or noise [14–16]. These results motivate us to design short directional couplers that are robust against systematic variations by making use of the analogy between weakly coupled waveguides and two-level systems [7]. In this paper, we shall design short and robust directional couplers against coupling coefficient/wavelength variations, by using perturbation theory analysis instead of iterations [6]. The spatially varying coupling coefficient and propagation constant mismatch can be engineered to realize the corresponding Hamiltonian by changing the waveguide spacing and waveguide width.

#214031 - $15.00 USD Received 13 Jun 2014; revised 17 Jul 2014; accepted 18 Jul 2014; published 28 Jul 2014

2. Model, dynamical invariant and optimzation

We consider a directional coupler consisting of two waveguides placed in proximity with propagation constants $\beta_+(z)$ and $\beta_-(z)$. The refractive index or geometry of the two waveguides are allowed to vary along the propagation direction z. Light is coupled into the device at $z=0$ and out at $z=L$. Under the scalar and paraxial approximation and assuming weak coupling, the changes in the guided-mode amplitudes in the individual waveguides $\mathbf{A}=[A_+,A_-]^T$ with propagation distance is described by coupled-mode equations as, $d\mathbf{A}/dz=-i\mathbf{H}_0(z)\mathbf{A}$, that is,

$$\frac{d}{dz}\begin{bmatrix} A_+ \\ A_- \end{bmatrix} = -i\begin{bmatrix} -\Delta & \Omega \\ \Omega & \Delta \end{bmatrix}\begin{bmatrix} A_+ \\ A_- \end{bmatrix}, \tag{1}$$

where $\Omega\equiv\Omega(z)$ (real) is the coupling coefficient, and $\Delta\equiv\Delta(z)=(\beta_-(z)-\beta_+(z))/2$ describes the degree of mismatch between the waveguides. Replacing the spatial variation z with the temporal variation t, Eq. (1) is equivalent to the time-dependent Schrödinger equation ($\hbar=1$) describing the interaction dynamics of a two-state system driven by a coherent laser excitation. In the following, we shall apply such quantum-optics analogy to describe the coupling dynamics of the directional coupler, and design the waveguide parameters Ω and Δ such that the coupler is robust against the variations of coupling coefficient and input wavelength.

We are aiming to optimize the coupling dynamics with respect to coupling coefficient/wavelength variations, by combining invariant-based inverse engineering and perturbation theory. For $\mathbf{H_0}(z)$ given by (1), a dynamical invariant $\mathbf{I}(z)$ may be parameterized as [17]

$$\mathbf{I}(z)=\frac{\kappa}{2}\begin{pmatrix} \cos\theta & \sin\theta e^{-i\beta} \\ \sin\theta e^{i\beta} & -\cos\theta \end{pmatrix}, \tag{2}$$

where $\theta\equiv\theta(z)$ and $\beta\equiv\beta(z)$ are z-dependent angles, κ is an arbitrary constant with units of mm^{-1}. Using the invariance condition, $\partial_t\mathbf{I}+(1/i)[\mathbf{I},\mathbf{H}_0]=0$ [18], we find the differential equations

$$\dot{\theta} = -\Omega\sin\beta, \tag{3}$$

$$\dot{\beta} = -\Omega\cot\theta\cos\beta-\Delta. \tag{4}$$

The eigenstates of the invariant can be written as

$$|\phi_+(z)\rangle=\begin{pmatrix} \cos(\theta/2)e^{-i\beta} \\ \sin(\theta/2) \end{pmatrix}, \tag{5}$$

$$|\phi_-(z)\rangle=\begin{pmatrix} \sin(\theta/2) \\ -\cos(\theta/2)e^{i\beta} \end{pmatrix}, \tag{6}$$

with eigenvalues $\lambda_\pm=\pm\Omega/2$. According to Lewis-Riesenfeld theory [18], the system state can be in general written as

$$|\Psi(z)\rangle=\Sigma_\pm c_\pm e^{i\gamma_\pm(z)}|\phi_\pm(z)\rangle, \tag{7}$$

where the $c_\pm$ are z-independent amplitudes, and Lewis-Riesenfeld phases $\gamma_\pm(z)$ must be the solution of

$$\dot{\gamma}_\pm(z)=\pm\frac{1}{2}\left(\dot{\beta}+\frac{\dot{\theta}\cot\beta}{\sin\theta}\right). \tag{8}$$

To achieve coupling between two waveguides by invariant engineering, the initial and final states of the system are set as $|\Psi(0)\rangle=|2\rangle\equiv\binom{0}{1}$ and $|\Psi(L)\rangle=|1\rangle\equiv\binom{1}{0}$ respectively. The

#214031 - $15.00 USD Received 13 Jun 2014; revised 17 Jul 2014; accepted 18 Jul 2014; published 28 Jul 2014

state trajectory between them may be parameterized according to one of the eigenstates of the invariant in Eq. (5). By using $|\phi_+(z)\rangle$, the boundary conditions [17]

$$\theta(0)=\pi, \quad \theta(L)=0, \tag{9}$$

guarantee the desired initial and final states. If in addition

$$\dot{\theta}(0)=0, \quad \dot{\theta}(L)=0, \tag{10}$$

then $\Omega(0)=\Omega(L)=0$, and $\mathbf{H}_0(z)$ and $\mathbf{I}(z)$ commute at input $z=0$ and output $z=L$. The commutativity at the boundaries implies that the operators share the eigenstates so, the input and output waveguide modes can transform into the eigenmodes of $\mathbf{I}(z)$ smoothly. There is still much freedom to design the coupling coefficient and detuning, see Eqs. (3) and (4), by choosing arbitrary functions θ and β except for boundary conditions. The freedom allows one to engineer stable or robust system evolution against different errors [14–16], which is not possible with the solution obtained by direct integration of Eq. (1).

Now, we first optimize the system stability against coupling coefficient variations, which can be simply described by the systematic error in Rabi frequency, that is, $\mathbf{H}_1=\delta\Omega(z)\sigma_x/2$, where σ_x is the Pauli spin matrix and δ is the amplitude of the relative error. Let the ideal, unperturbed Hamiltonian be $\mathbf{H}_0$ given by Eq. (1). In the error-free case, we consider the family of protocols that results in perfect state transfer from $|2\rangle$ to $|1\rangle$: the unperturbed solution, $|\Psi(z)\rangle=e^{i\gamma_+(z)}|\phi_+(z)\rangle$, satisfying Eq. (9). We shall consider H_1 as perturbation, and define the coupling coefficient-error sensitivity as [14]

$$q_\Omega=-\frac{1}{2}\frac{\partial^2 P_1(L)}{\partial\delta^2}\bigg|_{\delta=0}, \tag{11}$$

where P_1 is the probability to be in the state $|1\rangle$ at $z=L$, i.e. $P_1\approx 1-q_\Omega\delta^2$. By using perturbation theory, keeping the second order, we obtain

$$q_\Omega=\frac{1}{4}\left|\int_0^L dz\dot{\theta}\sin^2\theta e^{im(z)}\right|^2, \tag{12}$$

with $m(z)=2\gamma_+(z)-\beta(z)$. The minimum of q_Ω is achieved when q_Ω is nullified, which gives the maximal robustness with respect to coupling coefficient variations. Following [14], we can obtain $q_\Omega=\sin^2(n\pi)/(4n^2)$ by imposing $m(z)=n(2\theta-\sin 2\theta)$, so that $q_\Omega=0$ is achieved, if $n=1,2,3....$ In the case of $n=1$, we have

$$\beta=-\arctan(4\sin^3\theta), \tag{13}$$

which results in $q_\Omega=0$. As an example, we choose smooth function

$$\theta=\frac{\pi}{2}\left[1-\sin\frac{\pi(2z-L)}{2L}\right], \tag{14}$$

satisfying Eqs. (9) and (10). Substituting Eqs. (13) and (14) into Eqs. (3) and (4), we can solve for

$$\Omega = -\dot{\theta}/\sin\beta, \tag{15}$$

$$\Delta = -4\dot{\theta}\cos\theta\sin^2\theta-\dot{\beta}, \tag{16}$$

to achieve optimal coupling dynamics with respect to coupling coefficient variations.

#214031 - $15.00 USD Received 13 Jun 2014; revised 17 Jul 2014; accepted 18 Jul 2014; published 28 Jul 2014

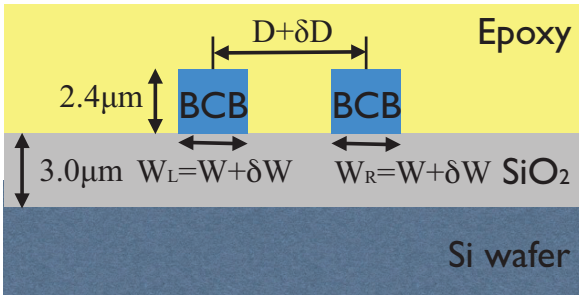

Fig. 1. Cross-sectional schematic of the polymer channel waveguide structure considered for device design.

Next, we target to design the robust couplers with respect to input wavelength variations. The dominant term affecting the spectral characteristic of a direction coupler is the variation of Δ against λ [5, 19], thus the input wavelength variations can be mainly described by the systematic error in detuning, $\mathbf{H}_2 = \delta\sigma_z/2$, where σ_z is the Pauli spin matrix and δ is a constant frequency shift. Similarly, we can define the wavelength-error sensitivity and finally obtain [16]

$$q_\Delta = \frac{1}{4}\left|\int_0^L dz \sin\theta e^{im(z)}\right|^2, \tag{17}$$

with $m(z) = 2\gamma_+(z) - \beta(z)$. To nullify q_Δ, i.e. $q_\Delta = 0$, we may assume $m(z) = 2\theta + 2\alpha\sin(2\theta)$, with free parameter α [16]. After some straightforward calculations, we obtain

$$\beta = \cos^{-1}\left(\frac{2M\sin\theta}{\sqrt{1+4M^2\sin^2\theta}}\right). \tag{18}$$

with $M = 1 + 2\alpha\cos(2\theta)$. Combining Eqs. (14) and (18), we solve for the design parameters as follows

$$\Omega = -\dot{\theta}\sqrt{1+4M^2\sin^2\theta}, \tag{19}$$

$$\Delta = 2\dot{\theta}\cos\theta\left[M + \frac{1-4\alpha+6\alpha\cos(2\theta)}{1+4M^2\sin^2\theta}\right], \tag{20}$$

which finally gives $q_\Delta = 0$ with the parameter $\alpha = -0.206$ and the smallest value of required coupling coefficient, $\Omega^{\max} = 14.784$.

3. Numerical simulations

We illustrate the design of directional couplers using shortcuts to adiabaticity in a conventional planar integrated optics platform and perform beam propagation method (BPM) simulations to verify the designs. The cross-section of the polymer channel waveguide structure is shown schematically in Fig. 1. The design parameters are chosen as follows: 3 μm thick SiO_2 (n =1.46) on a Si ($n = 3.48$) wafer is used for the bottom cladding layer, the core consists of a 2.4 μm layer of BCB ($n = 1.53$), and the upper cladding is epoxy ($n = 1.50$). This weakly-guided coupled waveguide structure can be well-described by the scalar and paraxial wave equation, and the evolution of the guided modes in the coupler can be accurately described by Eq. (1). The BPM code solves the the scalar and paraxial wave equation using the

#214031 - $15.00 USD Received 13 Jun 2014; revised 17 Jul 2014; accepted 18 Jul 2014; published 28 Jul 2014

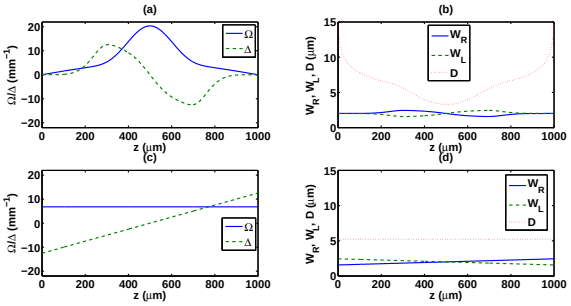

Fig. 2. Coupling coefficient Ω and detuning Δ variation along z for the coupler designs. (a) Ω-coupler. (c) adiabatic coupler. The corresponding waveguide parameters. (b) Ω-coupler. (d) adiabatic coupler.

finite difference scheme with the transparent boundary condition [20]. The devices are simulated at 1.55 μm input wavelength and the TE polarization. Subsequent waveguide design and BPM simulations are performed on the 2D structure obtained using the effective index method. For the coupler design, the default width for the right and left waveguides is chosen to be $W_R = W_L = 2$ μm. Through BPM simulations, we verified that the relation between the mismatch Δ and width difference δW can be approximated by a linear relation [1], and the relation between the coupling coefficient Ω and waveguide separation D in a symmetric coupler is well fitted by the exponential relation $\Omega = \Omega_0 \exp[-\gamma(D - D_0)]$ [21]. We also assume that the exponential relation can be used to obtain an estimation of the coupling coefficient in the asymmetric coupler [1]. The waveguide spacing $D(z)$ and width difference $\delta W(z)$ are then adjusted along the propagation direction to satisfy the designed set of $\Omega(z)$ and $\Delta(z)$ functions.

3.1. Ω-coupler

First, we design a directional coupler that is robust against coupling coefficient variations (Ω-coupler) using Eqs. (15) and (16) at a length of L =1 mm. Figure 2(a) shows the calculated coupling coefficient Ω and detuning Δ. Using the exponential relation between Ω and D and the linear relation between Δ and δW, we obtain the corresponding waveguide parameters W_R, W_L, and D as a function of z as shown in Fig. 2(b). The geometry of the designed directional coupler is shown in Fig. 3(a). We also design an adiabatic coupler of the same length using the linearly tapered mismatch profile [2, 22] with a constant coupling coefficient Ω and a linearly varying detuning Δ shown in Fig. 2(c). We choose the constant coupling coefficient of the adiabatic coupler such that the area under the Ω curves in Figs. 2(a) and (c) are equal, and the maxima and minima of the Δ curves in the same figures are equal. The resulting waveguide parameters and the corresponding waveguide geometry of the adiabatic coupler are shown in Fig. 2(d) and Fig. 3(b), respectively. Finally, we also design a resonant directional coupler at the same length using the resonant coupling scheme with two parallel waveguides as shown in Fig. 3(c) for comparison.

For the devices in Fig. 3, we excite the lower (righthand side in Fig. 1) waveguides by their unperturbed mode at $z = 0$ with a input wavelength of 1.55 μm, and the BPM results are shown in the same figures. Power is coupled completely to the upper waveguide for the Ω-coupler in Fig. 3(a) and the resonant coupler in Fig. 3(c). For the adiabatic coupler in Fig. 3(b), the power coupling is incomplete because the adiabatic condition has not been met. For the chosen design parameters, we plot the conversion efficiency as a function of the device length L (interaction length) for the three coupler designs in Fig. 4. It is clear that the adiabatic coupler length needs

#214031 - $15.00 USD Received 13 Jun 2014; revised 17 Jul 2014; accepted 18 Jul 2014; published 28 Jul 2014

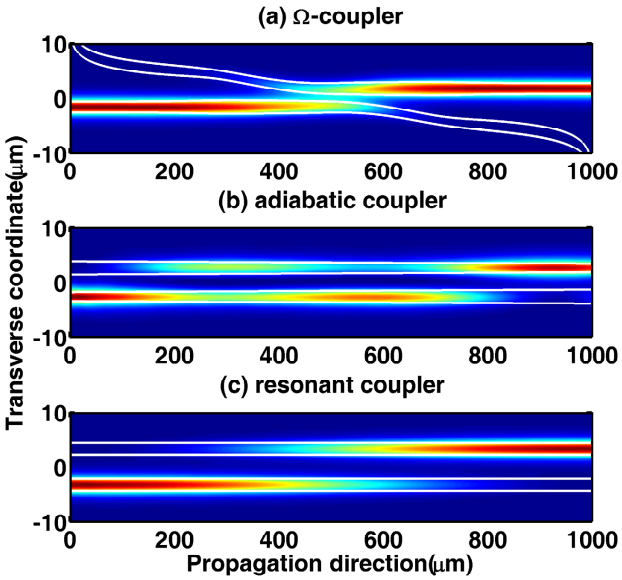

Fig. 3. Waveguide geometries and the corresponding beam propagation simulations for (a) Ω-coupler, (b) adiabatic coupler, and (c) resonant coupler. White lines indicate the waveguide cores.

to satisfy $L \geq 1.5$ mm in order to have minimized coupling between the supermodes. Even with the increased device length, we still observe oscillatory behavior in the coupling efficiency, which is characteristic of adiabatic devices due to finite coupling between the supermodes. So, complete power coupling can only happen at specific device lengths. On the other hand, the Ω-coupler exhibits optimized tolerance to device length (interaction length) variations around the designed length of 1 mm. The resonant coupler exhibits the expected sinusoidal behavior with device length change.

To investigate the device robustness against coupling coefficient variations, we vary the spacing between the waveguides (δD in Fig. 1(a)) in BPM simulations and show the resulting coupling efficiencies as a function of δD in Fig. 5. The Ω-coupler design exhibits the desired flatness around $\delta D = 0$ as a result of our optimization of the perturbation theory result, see Eq. (12), by using invariant-based inverse engineering. The invariant based design clearly shows better tolerance to coupling coefficient variations at a shorter length than a conventional tapered mismatched adiabatic coupler and the resonant coupler.

We also look at the robustness of the Ω-coupler against refractive index variations. We vary the difference between the core and cladding effective indices Δn from -75 % to +75 % in our BPM simulations and compare the coupling efficiencies of the three devices in Fig. 6. The Ω coupler shows flat response against refractive index difference variations, while the adiabatic coupler and the resonant coupler show the expected oscillatory behavior. So far, we have examined the robustness of the Ω-coupler against device length variations as well as against coupling coefficient variations resulting from waveguide spacing errors and refractive index variations. Overall, the Ω-coupler shows the desired robustness against errors in Ω in Eq. (1) at a short device length, as a result of our optimization.

#214031 - $15.00 USD Received 13 Jun 2014; revised 17 Jul 2014; accepted 18 Jul 2014; published 28 Jul 2014

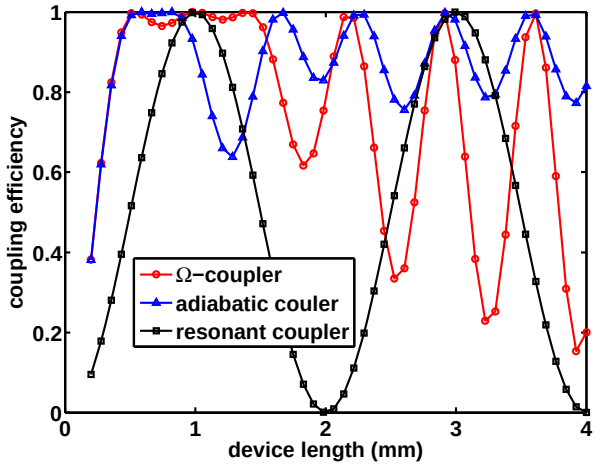

Fig. 4. Coupling efficiencies as a function of device length L.

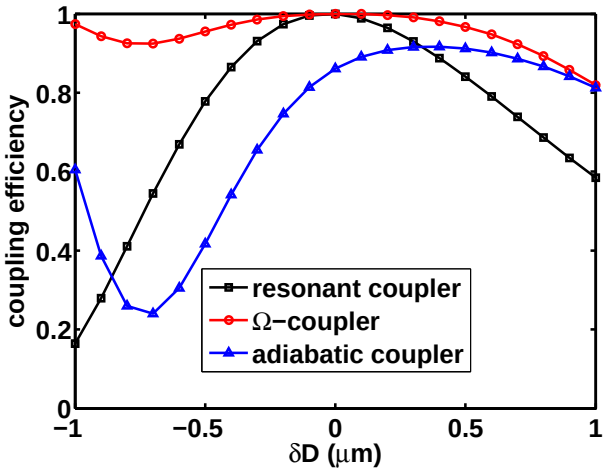

Fig. 5. Coupling efficiencies as a function of waveguide spacing error δD

#214031 - $15.00 USD Received 13 Jun 2014; revised 17 Jul 2014; accepted 18 Jul 2014; published 28 Jul 2014

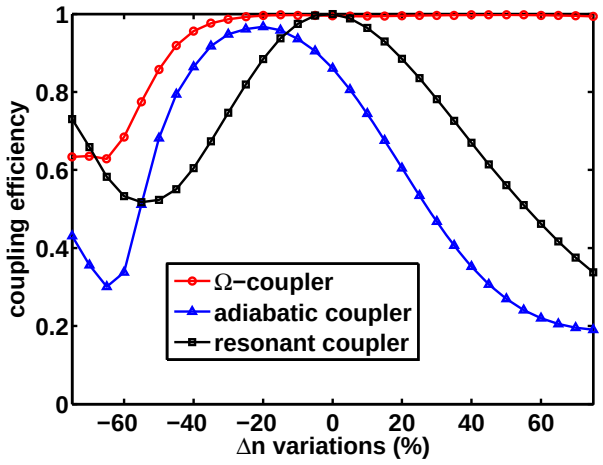

Fig. 6. Coupling efficiencies as a function of refractive index variations.

3.2. Δ-coupler

Next, we apply the optimal protocol for robustness against wavelength variations (Δ-coupler), obtained from Eqs. (19) and (20) to design a coupler at a length of $L = 1$ mm. Figures 7(a) and (b) shows the calculated Ω, Δ and the corresponding waveguide parameters. Figure 8(a) shows the geometry of the designed device. Again, we also design an adiabatic coupler using the linearly tapered mismatch profile with a constant coupling coefficient such that the area under the Ω curves in Figs. 7(a) and (c) are equal, and the maxima and minima of the Δ curves in the same figures are equal. The resulting waveguide parameters and the corresponding waveguide geometry of the adiabatic coupler are shown in Fig. 7(d) and Fig. 8(b), respectively. We excite the lower waveguides by their unperturbed mode at $z = 0$ with a input wavelength of 1.55 μm, and the BPM results are shown in the same figures. Power is coupled completely to the upper waveguide for the Δ-coupler in Fig. 8(a), and the coupling efficiency is 0.96 for the adiabatic coupler in Fig. 8(b). The power coupling is incomplete in the adiabatic coupler because its coupling efficiency exhibits similar oscillatory behavior as a function of the device length as shown in Fig. 4. For the chosen design parameter, we find that the device length needs to satisfy $L \geq 1.7$ mm in order to have minimized coupling between the supermodes.

We then vary the input wavelength from 1 μm to 2 μm with 0.05 μm steps in BPM simulations, and material dispersion in the waveguide is not considered. The resulting coupling efficiency spectra for the Δ-coupler and the adiabatic coupler in Fig. 8, as well as for the resonant coupler in Fig. 3(c), are shown in Fig. 9. The spectrum of the Δ-coupler design exhibits the desired flatness around the zero-detuning wavelength of 1.55 μm. The adiabatic coupler exhibits broadband response as compared to the resonant coupler, although still narrower than the optimized Δ-coupler. The oscillation with wavelength is also characteristic of an adiabatic coupler. The spectrum of the resonant coupler shows the expected sinusoidal variation [21]. The robustness of the Δ-coupler is superior to that of the adiabatic coupler and the resonant coupler as expected, and the robustness is achieved at a shorter length than a conventional tapered mismatched adiabatic coupler. In fact, more stable schemes can be further designed by cancelling higher orders of the perturbations approximation [15].

#214031 - $15.00 USD Received 13 Jun 2014; revised 17 Jul 2014; accepted 18 Jul 2014; published 28 Jul 2014

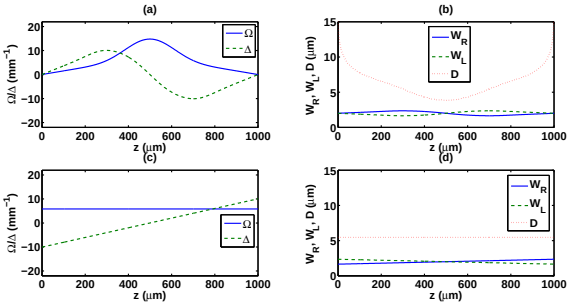

Fig. 7. Coupling efficiency Ω and detuning Δ variation along *z* for the coupler designs. (a) Δ-coupler. (c) adiabatic coupler. The corresponding waveguide parameters. (b) Δ-coupler. (d) adiabatic coupler.

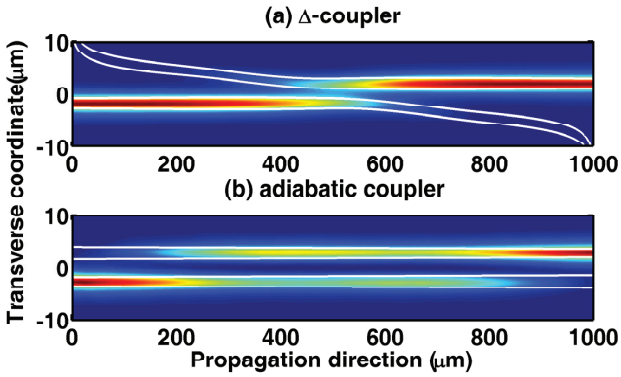

Fig. 8. Waveguide geometries and the corresponding beam propagation simulations for (a) Δ-coupler and (b) adiabatic coupler. White lines indicate the waveguide cores.

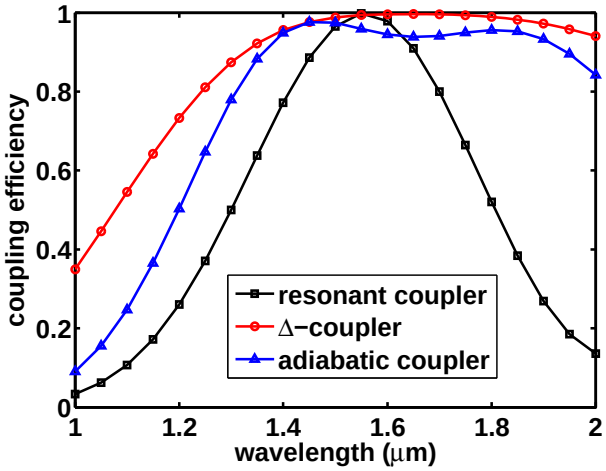

Fig. 9. Coupling efficiencies as a function of input wavelength.

#214031 - $15.00 USD Received 13 Jun 2014; revised 17 Jul 2014; accepted 18 Jul 2014; published 28 Jul 2014

4. Discussion and conclusion

From the theoretical analysis and numerical simulations, we can see that the adiabatic design offers high coupling efficiency when the device length is sufficiently long to satisfy the adiabatic condition but does not guarantee complete power coupling at the designed device length due to coupling efficiency oscillations resulting from finite coupling between the supermodes. The adiabatic design offers better robustness against coupling coefficient/wavelength variations then the resonant coupler, however, the device robustness would depend on the chosen shape functions [1,2]. On the other hand, the invariant-based inverse engineering approach guarantees complete power coupling in a direction coupler at the designed device length, as a result of the boundary conditions we set at the input and output of the coupler. When combined with the perturbation theory, the invariant-based approach can be used to optimize the device robustness against the chosen error, resulting in robust directional couplers at shorter lengths then the adiabatic devices. The device robustness against errors exhibits asymmetries around the designed values, which is similar to the characteristic of the adiabatic devices; but the adiabaticity of the device is achieved at a shorter device length via the invariant-based shortcut, with guaranteed perfect power coupling at zero error.

In conclusion, we demonstrated that the invariant-based inverse engineering approach can be applied successfully to waveguide directional coupler design. Combined with perturbation treatment of the coupled mode equations, we use the approach to design directional couplers that are robust against coupling coefficient/wavelength variations. The invariant-based analysis provides a quick and straightforward approach to optimize the device performance. The design parameters are applicable to weakly coupled devices in general.

Acknowledgments

This work was supported in part by the MOST of Taiwan (103-2221-E-006-055 and 103-3113-M-110-001), NSFC (61176118), the Shanghai Rising-Star and Pujiang Program (Grant Nos. 12QH1400800 and 13PJ1403000), the Specialized Research Fund for the Doctoral Program (Grant No. 2013310811003), and the Program for Professor of Special Appointment (Eastern Scholar) at Shanghai Institutions of Higher Learning.

#214031 - $15.00 USD Received 13 Jun 2014; revised 17 Jul 2014; accepted 18 Jul 2014; published 28 Jul 2014